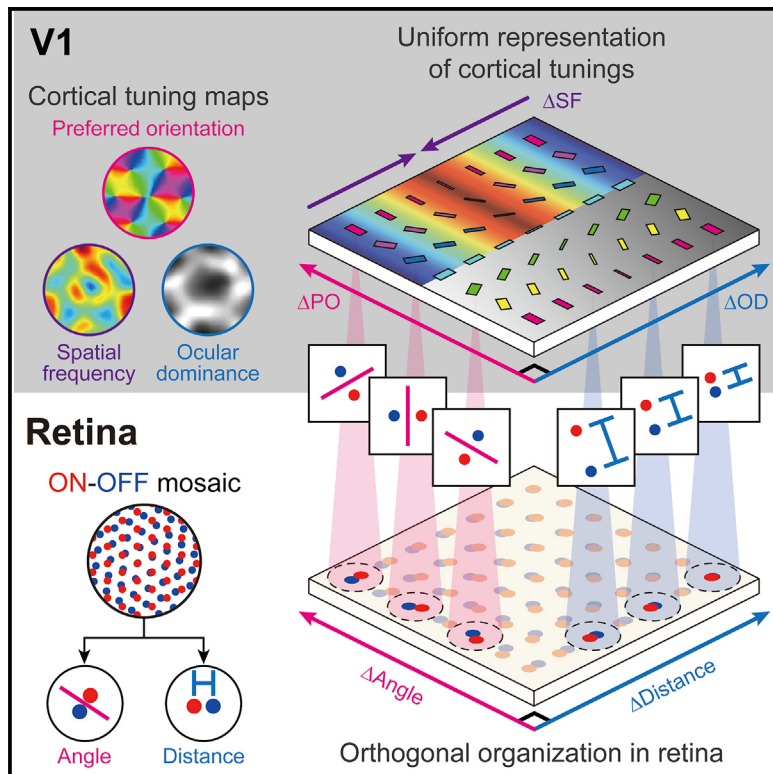


Projection of Orthogonal Tiling from the Retina to the Visual Cortex

Graphical Abstract



Authors

Min Song, Jaeson Jang, Gwangsu Kim,
Se-Bum Paik

Correspondence

sbpaik@kaist.ac.kr

In Brief

In higher mammals, the primary visual cortex is organized into diverse tuning maps of visual features, the topography of which intersects orthogonally. Here, Song et al. propose that the regularly structured retinal circuits initiate the clustered topography of multiple tuning maps for the efficient tiling of functional domains in visual cortex.

Highlights

- Orthogonal organization of visual tuning maps is observed in both V1 and the retina
- Cortical tuning maps are correlated with the profile of ON-OFF feedforward projections
- The profile of ON-OFF receptive fields varies periodically across the V1 and retina
- Regularly structured retinal mosaics initiate the orthogonal tiling of the V1



Report

Projection of Orthogonal Tiling from the Retina to the Visual Cortex

Min Song,^{1,2,4} Jaeson Jang,^{1,4} Gwangsu Kim,³ and Se-Bum Paik^{1,2,5,*}

¹Department of Bio and Brain Engineering, Korea Advanced Institute of Science and Technology, Daejeon 34141, Republic of Korea

²Program of Brain and Cognitive Engineering, Korea Advanced Institute of Science and Technology, Daejeon 34141, Republic of Korea

³Department of Physics, Korea Advanced Institute of Science and Technology, Daejeon 34141, Republic of Korea

⁴These authors contributed equally

⁵Lead Contact

*Correspondence: sbpaik@kaist.ac.kr

<https://doi.org/10.1016/j.celrep.2020.108581>

SUMMARY

In higher mammals, the primary visual cortex (V1) is organized into diverse tuning maps of visual features. The topography of these maps intersects orthogonally, but it remains unclear how such a systematic relationship can develop. Here, we show that the orthogonal organization already exists in retinal ganglion cell (RGC) mosaics, providing a blueprint of the organization in V1. From analysis of the RGC mosaics data in monkeys and cats, we find that the ON-OFF RGC distance and ON-OFF angle of neighboring RGCs are organized into a topographic tiling across mosaics, analogous to the orthogonal intersection of cortical tuning maps. Our model simulation shows that the ON-OFF distance and angle in RGC mosaics correspondingly initiate ocular dominance/spatial frequency tuning and orientation tuning, resulting in the orthogonal intersection of cortical tuning maps. These findings suggest that the regularly structured ON-OFF patterns mirrored from the retina initiate the uniform representation of combinations of map features over the visual space.

INTRODUCTION

In higher mammals, the primary visual cortex (V1) is organized into various functional maps of neural tuning such as ocular dominance (OD) (LeVay et al., 1985), preferred orientation (PO) (Blasdel and Salama, 1986), and spatial frequency (SF) (Movshon et al., 1978) (Figure 1A). Interestingly, the topographies of the observed functional maps are precisely correlated, implying uniform coverage of sensory modules in the visual space. For instance, it was reported that the gradient of orientation tuning intersects orthogonally with that of OD or preferred SF in the same cortical area in cats (Hübener et al., 1997) and in monkeys (Nauhaus et al., 2012) (Figure 1B). High-resolution two-photon imaging data revealed that the region of higher SF tuning tends to align with the binocular region in the OD map in monkeys (Nauhaus et al., 2016). Although the role of each functional map is under debate (Van Hooser, 2007; Horton and Adams, 2005), such structural correlations between maps are thought to result in the uniform representation of visual features across cortical areas, enabling the sampling of a complete set of functional tunings regardless of where the visual space is (Swindale et al., 2000) (Figure 1C).

Furthermore, observed correlations between different functional maps have raised the possibility that there exists a common principle of developing individual functional maps and their systematic organization (Nauhaus and Nielsen, 2014). Important clues regarding the development of the maps have been found in the observation that cortical tuning, such as orientation selec-

tivity, may originate from bottom-up feedforward projections. Although feedforward thalamic inputs are a small portion of the total inputs (Douglas et al., 1995), earlier work reported that the orientation tuning of V1 neurons originates from this feedforward pathway and the orientation preference of a V1 neuron remains consistent when the recurrent cortical circuits are silenced (Chung and Ferster, 1998; Ferster et al., 1996). Recently, it was reported that orientation tuning in V1 is predictable from the local average of ON and OFF thalamic afferents (Jin et al., 2011) (Figure 1D). At larger scales, it was also reported that the continuous change of orientation tuning across the cortical surface is strongly correlated with the spatial alignment of ON and OFF receptive fields in cats and tree shrews (Kremkow et al., 2016; Lee et al., 2016). These observations suggest that visual tuning in the cortical neurons may originate from the spatial organization of ON and OFF feedforward afferents, and map structures of cortical tuning may also be seeded initially from thalamic feedforward projections.

Computational model studies also suggested that the functional tuning in V1 is constrained by the local structure of ON and OFF mosaics of retinal ganglion cells (RGCs) (Ringach, 2004, 2007; Soodak, 1987). Our previous studies successfully explained how regularly structured cell mosaics in the retina could seed the early structure of an orientation map (Jang et al., 2020; Paik and Ringach, 2011, 2012). In this scenario, the receptive field of a V1 neuron is generated from the sum of receptive fields of local RGCs that provide feedforward inputs, and the V1 neuron is tuned to visual features due to the anisotropy of the receptive fields (Figure 1E, pink arrows). These results



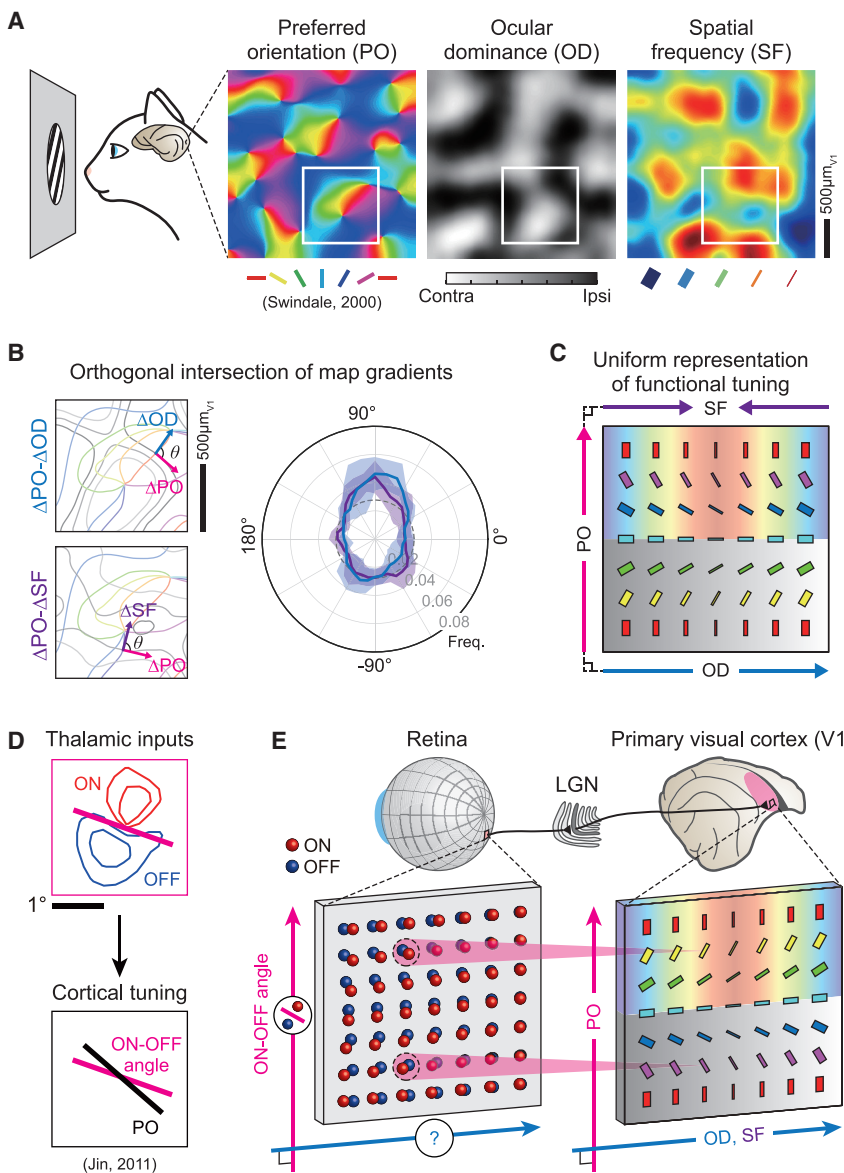


Figure 1. Orthogonal Organization of Diverse Cortical Tunings in Visual Cortex

(A) Functional tuning maps in the visual cortex of higher mammals.

(B) Orthogonal relationship between the gradients of diverse cortical tuning maps (Nauhaus et al., 2012, 2016; Swindale et al., 2000). Inset, contours of orientation tuning (colored lines) and ocular dominance/spatial frequency (OD/SF) tuning (gray lines) from the area in white squares in (A). The shaded area indicates SD.

(C) Uniform representation of diverse tunings is illustrated.

(D) Orientation tuning in V1 predicted from the local average of ON and OFF thalamic afferents.

(E) Illustration of the predicted relationship between the spatial arrangement of ON and OFF RGCs and cortical tunings.

cortex and that this common anatomical substrate results in the uniform representation of combinations of sensory modules by organizing the topographical correlations between diverse tunings. As expected, our analysis of published V1 recording data measured in cats (Kremkow et al., 2016) shows that the OD and SF in V1 are correlated with the spatial separation of the ON and OFF subdomains of the receptive fields (Figure 3), as predicted by our model simulation (Figure 4). By combining our analyses of data in distinct species and model simulations, we demonstrate that the regularly structured retinal circuits provide a common framework of various functional maps and topographic correlations among the maps in V1.

RESULTS

Orthogonal Organization of ON and OFF RGCs

From the observation of the correlation between the ON-OFF angle in the retinal afferents

and the cortical orientation tuning, we hypothesized that other cortical tunings may also be predictable from a profile of the spatial arrangement of ON and OFF RGCs, which can be expected to change orthogonally with a change in the ON-OFF angle across the retinal mosaics. In this scenario, this spatial organization of ON and OFF RGCs is mirrored to V1 and induces orthogonal tiling of a neural tuning (Figure 1E). To validate this scenario, we used RGC mosaics data previously measured in cats (Zhan and Troy, 2000) (Figure 2A, left) and examined whether a change of the angle and distance between the local ON and OFF RGC mosaics would have an orthogonal organization.

Based on the statistical wiring model (Ringach, 2007), we estimated the ON-OFF angle and distance of the sampled receptive field at each position of the RGC mosaics while assuming that RGCs are locally sampled to provide feedforward afferents in the local V1 area (Figures 2A and 2B, left). In this model,

suggested that simple feedforward wiring from the periphery can provide a strategy to build the initial circuitry for sensory function in V1. However, how the topographic maps of multiple neural tunings arise in V1 and how such a systematic relationship of maps can be achieved in parallel with the development of each map (Figure 1E, blue arrows) are still poorly understood.

Here, we show that an orthogonal relationship of tuning modules already exists in retinal mosaics and that this can be mirrored to V1 to initiate the clustered topography of multiple tuning maps. From an analysis of RGC mosaics data in cats and monkeys, we found that the topographic map of spatial separation of the ON and OFF RGCs (ON-OFF distance) intersects orthogonally with the map of ON-OFF alignment angles (ON-OFF angle) (Figure 2). Our model simulations suggest that these regularly structured retinal afferents can provide a common framework for organizing various functional maps in the visual

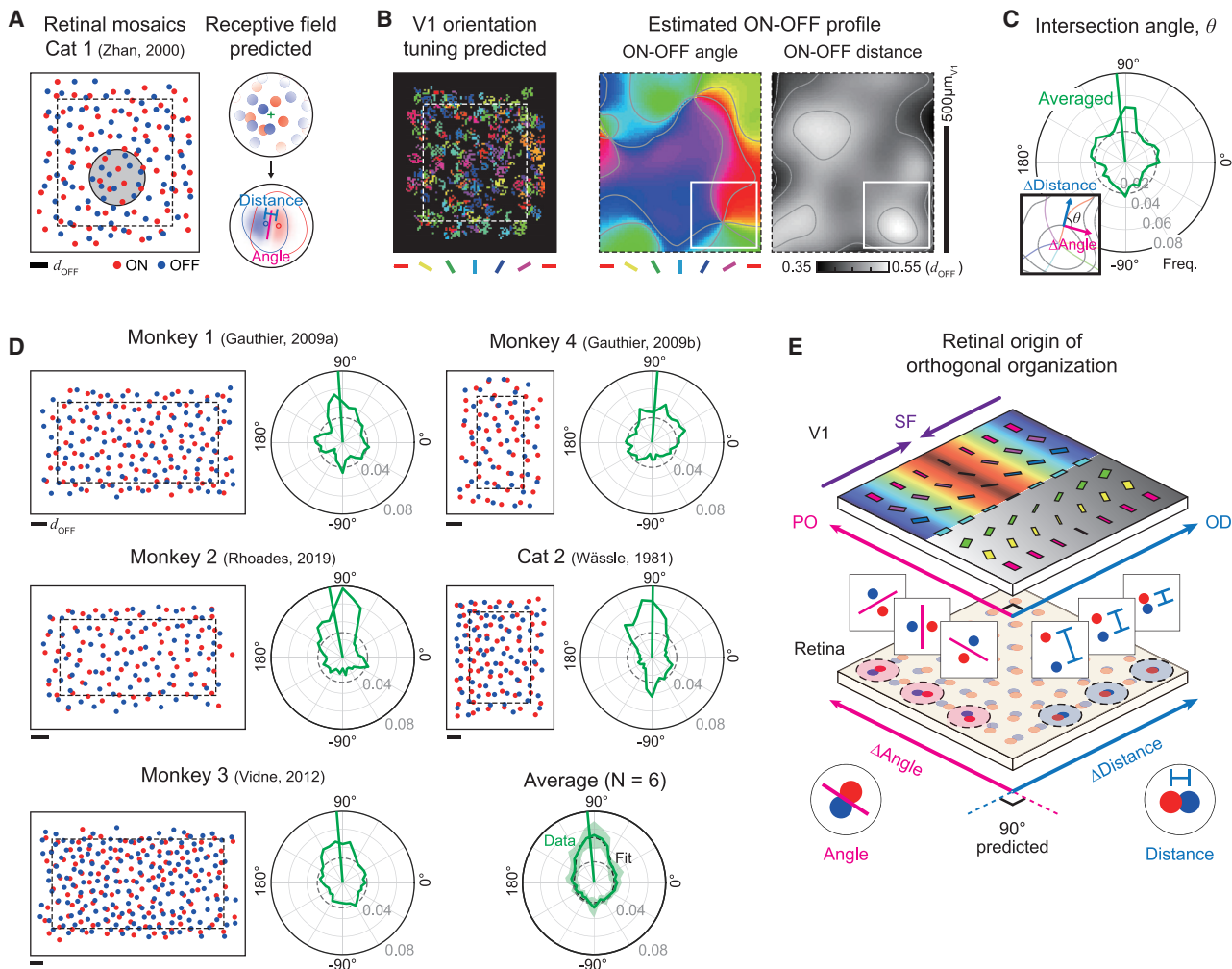


Figure 2. Orthogonal Organization between ON-OFF Angle and Distance in RGC Mosaics

- (A) Estimation of angle and distance between local ON and OFF receptive fields from the measured RGC mosaics.
 - (B) Left: ON-OFF angle measured from the RGC mosaics. Center and right: smoothed maps for gradient analysis (within the black dashed square in A). (C) Orthogonal intersection between gradients of ON-OFF angle and distance. Green arrows indicate the average intersection angle. Inset, contours of ON-OFF angle (colored lines) and distance (gray lines) in the white solid square in smoothed maps.
 - (D) Similar analyses for 5 other RGC mosaic datasets. Scale bar, the expected average lattice distance of OFF mosaics, d_{OFF} . Gray dashed lines indicate the chance level. The shaded area indicates SD.
 - (E) This orthogonal organization in the retina can be mirrored to V1 and induces orthogonal tiling of a neural tuning.
- See also Figure S1.

neighboring cortical neurons can sample a similar RGC population but generate a different orientation preference, depending on the set of several RGCs that provide the dominant inputs to the neuron. We calculated the angle of the intersection between the gradients of the ON-OFF angle and that of the distance in smoothed maps (Figure 2B, center and right). The smoothed map of the ON-OFF angle covers approximately one period of the columnar structure and is thus comparable to the estimation obtained from the size of the RGC mosaics and the retinocortical magnification factor (Jang et al., 2020). As predicted by our scenario, we found that the angle shows a peak at ~90° (Figure 2C).

We repeated this analysis for 5 sets of RGC mosaic data of different eccentricities, obtained from independent experiments, in multiple species ($N = 2$ for cat [Wässle et al., 1981; Zhan and Troy, 2000]; $N = 4$ for monkey [Gauthier et al., 2009a, 2009b; Rhoades et al., 2019; Vidne et al., 2012]) and confirmed the orthogonal intersection between the ON-OFF angle and distance in all sets of tested data (Figure 2D). Each mosaic sample and the average distribution of all datasets showed a peak at 90°, significantly higher than that of the control sets with the shuffled distribution of the ON-OFF angle and distance (Figure 2D bottom right; fitted to a von Mises distribution, ON-OFF angle and distance, $\mu = 92.4^\circ$, $\kappa = 5.34$, control, $n = 1,000$, $\kappa = 0.07 \pm 0.02$, ON-OFF angle

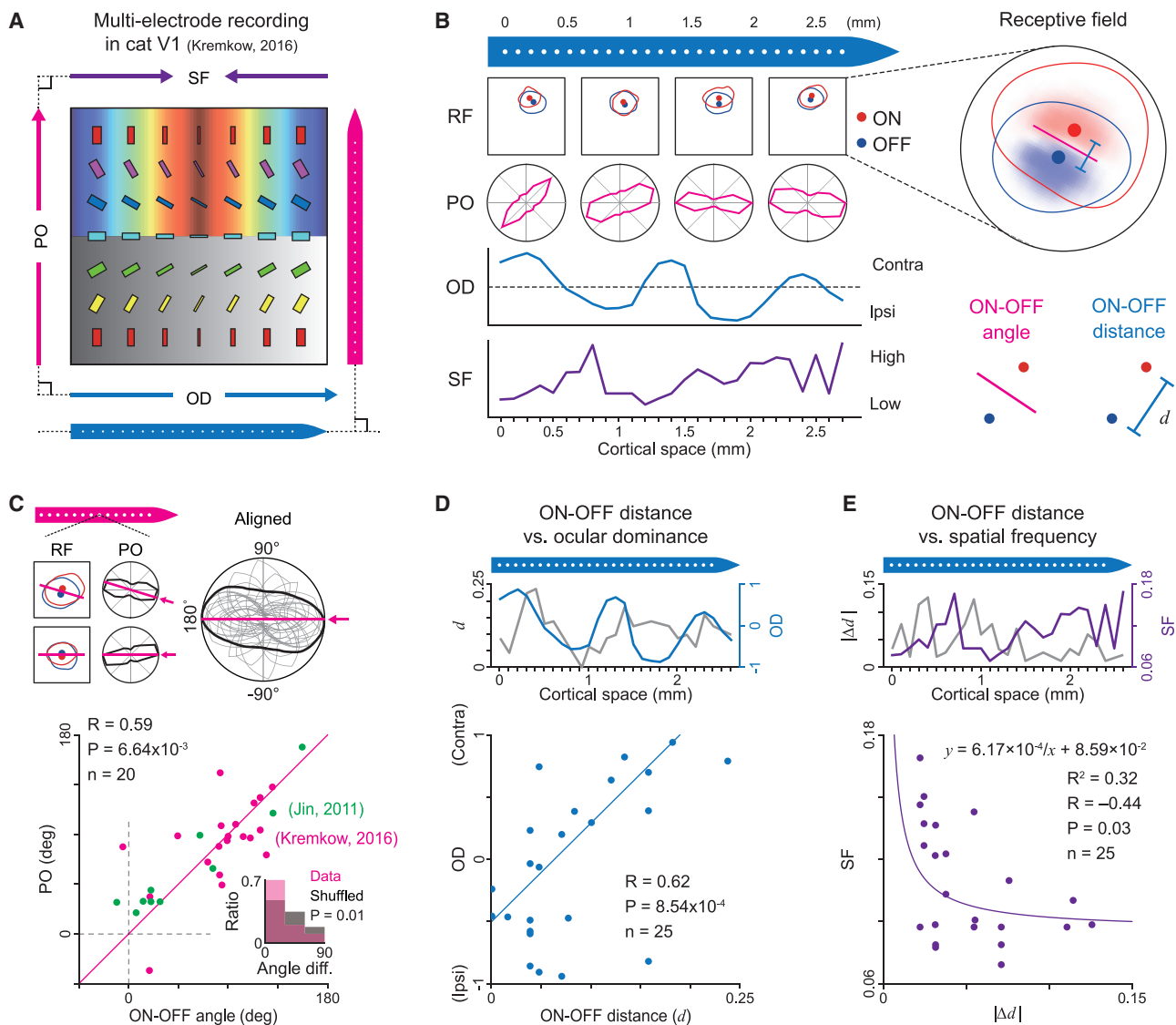


Figure 3. Topographic Correlation between ON-OFF Angle/Distance and Diverse Cortical Tunings

(A) Left: receptive fields and functional tunings were recorded by the electrodes penetrating cat V1 (modified from Figure 2B of Kremkow et al., 2016).
(B) ON-OFF angle and distance measured from the receptive fields.
(C) Top: ON-OFF angle estimated from the local receptive field is correlated with the orientation tuning measured at each electrode with $N = 20$ data points. Bottom: correlation between the ON-OFF angle and the preferred orientation (PO). Green solid circles indicate the data adapted from Jin et al. (2011). Inset: angle difference between the 2 angles. The average difference is significantly smaller than that of the shuffled pairs ($p = 0.01$, $N = 1,000$ repeated trials).
(D) Top: ON-OFF distance (d) and OD vary periodically across the cortical surface. Bottom: correlation between d and OD.
(E) Top: the deviation of ON-OFF distance from its average ($|\Delta d|$) and the SF tuning measured by the same electrode. Bottom: negative correlation between the preferred SF and $|\Delta d|$. The collected data were fitted with the $1/|\Delta d|$ function ($SF = 6.17 \times 10^{-4}/|\Delta d| + 8.59 \times 10^{-2}$).
(C-E) The correlation coefficient and their p-value were calculated from the Pearson's correlation.

and distance versus control, $p < 0.01$). Notably, the strength of this orthogonal bias is comparable to that observed in the cortex (orthogonality index [OI] = 3.35 ± 0.90 in the RGC mosaic; $OI_{\Delta PO-\Delta OD} = 3.90 \pm 3.3$ and $OI_{\Delta PO-\Delta SF} = 2.72 \pm 2.51$ in our analysis of V1 tuning shown in Figure 1A; fitted to a von Mises distribution, $\mu_{\Delta PO-\Delta OD} = 91.4^\circ$, $\kappa_{\Delta PO-\Delta OD} = 5.78$, $\mu_{\Delta PO-\Delta SF} = 89.8^\circ$, $\kappa_{\Delta PO-\Delta SF} =$

5.12), implying that the orthogonal bias observed in V1 may be projected from that in the RGC mosaics. These results show that the ON-OFF angle and distance in RGC mosaics intersect orthogonally across retinal space and this may provide the blueprint of orthogonal organization of functional tuning maps in V1 (Figures 2E and S1).

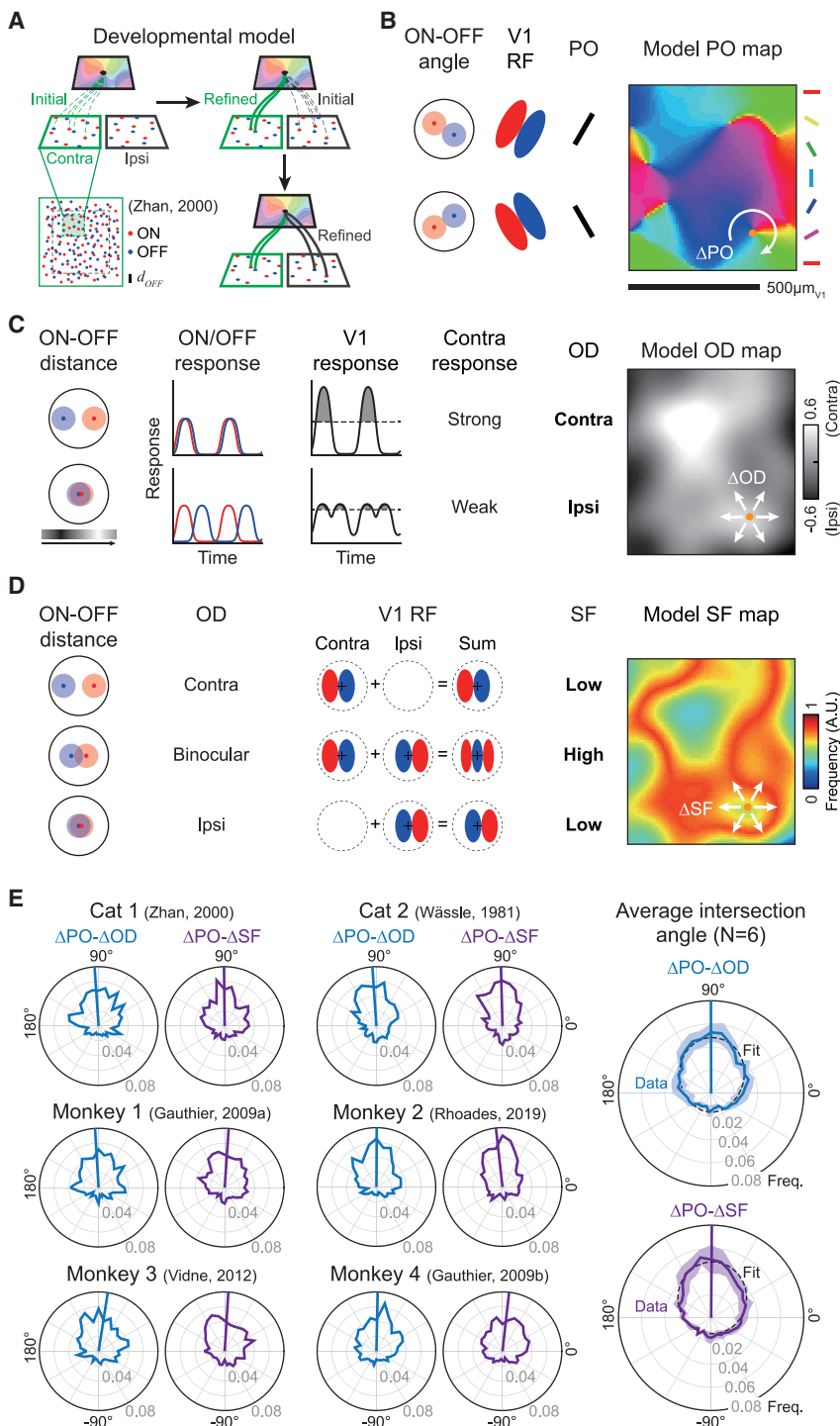


Figure 4. Retinal Origin of Orthogonal Organization of Cortical Tunings

(A) Sequential developmental model of contralateral and ipsilateral visual pathways.

(B–D) Developmental model of functional tunings from the feedforward projections of ON and OFF RGCs.

(B) By pooling local RGCs, orientation tuning of V1 neurons is constrained by ON-OFF angle alignment.

(C) OD is constrained by ON-OFF distance. According to the distance between neighboring RGCs in the contralateral retina, the degree of overlap between ON and OFF subregions in V1 receptive fields varies and differential response occurs. When ON and OFF subregions are far from each other, the V1 neuron can generate a strong response to contralateral input and become a contradominant cell. If ON and OFF RGCs are close, they are not simultaneously activated and cannot respond strongly to contralateral inputs and become ipsidominant cells.

(D) SF tuning is constrained by the balance between contralateral and ipsilateral inputs. In binocular regions, phase difference between the contralateral and ipsilateral receptive fields induces preference for higher SF.

(E) Top: the angle distribution of gradient intersection between orientation and OD maps (blue solid curve) or SF maps (violet solid curve) shows a peak at ~90° in the predicted cortical map from data retinal mosaics. Bottom: average of the angle distribution. The shaded area indicates SD.

The development of orthogonal bias in RGC mosaics was previously predicted by the Paik-Ringach model (Paik and Ringach, 2011). In earlier work, based on observations of long-range hexagonal periodicity and the difference between the ON-ON and OFF-OFF distances in data mosaics (Figures S1A–S1D), the model suggests that the superposition of ON and OFF RGCs generates an

interference pattern that initiates a periodic pattern of orientation maps; due to the organized arrangement of RGCs in this geometric pattern, the orthogonal relationship between the ON-OFF angle and distance arises spontaneously (Figures S1E and S1F). In addition, the orthogonal relationship is consistently obtained across different conditions of the lattice distance ratio (α) and the alignment angle (θ), and even obtained in the model-generated RGC mosaics with realistic noise level that observed in the measured RGC mosaics (Jang and Paik, 2017) (Figures S1G–S1J). These results suggest that ON and OFF RGC mosaics, with a certain level of spatial regularity as observed in various datasets, is likely to induce a correlated topography of the ON-OFF angle and distance.

Correlation between ON-OFF Afferents and Cortical Tunings

If the orthogonal tiling of tuning maps in the visual cortex originates from the spatial organization of ON-OFF afferents, then it is expected that the spatial separation of ON-OFF receptive fields (ON-OFF distance) must be correlated topographically

with the OD and SF tuning in V1 (Figure 2E). To test this prediction of the correlation between the ON-OFF distance and the OD/SF tuning (Figure 3A), we analyzed recently published cat data (Kremkow et al., 2016), in which the profile of V1 receptive fields and functional tuning were measured together across the cortical surface (Figure 3B, left). In this dataset, measurements from two electrodes parallel or perpendicular to an OD column enabled an analysis of the relationship between the cortical receptive fields and the underlying cortical tuning (red and blue electrodes in Figure 3A). From the observed receptive fields, we measured the angle and the distance between the center of ON and OFF subfields (Figure 3B, right) and examined correlations with underlying functional tunings.

We found that previously reported correlations between different functional tunings were confirmed with the current dataset. As in previous studies (Jin et al., 2011; Kremkow et al., 2016; Lee et al., 2016), we observed that orientation tuning is predicted by the angle between the ON and OFF receptive fields (ON-OFF angle; Figure 3C, $n = 20$, $R = 0.59$, $*p = 6.64 \times 10^{-3}$). Similarly, a correlation between binocularity ($1-|OD|$) and SF tuning (Nauhaus et al., 2016) was also observed ($n = 25$, $R = 0.41$, $*p = 0.03$), suggesting that this dataset represents profiles that can be used to validate our model prediction of the organization of a correlated topography in the visual cortex.

As predicted, we found that the distance between ON and OFF centers (ON-OFF distance, d) periodically changes across the cortical surface (Figure 3D, top). Notably, the spatial period of the ON-OFF distance variation was practically identical to that of the OD in the same cortical area (~2.9% difference; fitted to a sine curve). As a result, the observed OD appeared to correlate strongly to the ON-OFF distance (Figure 3D, bottom, $n = 25$, $R = 0.62$, $*p = 8.54 \times 10^{-4}$).

The ON-OFF distance and SF tuning were also systematically correlated in the same data. We found that the deviation of the ON-OFF distance from its average ($|\Delta d|$; Figure 3E, top, gray) is correlated negatively with SF tuning estimated from the fast Fourier transform (FFT) analysis of V1 receptive fields (Figure 3E, bottom, $n = 25$, $R = -0.44$, $*p = 0.03$). Considering the correlation between the OD and ON-OFF distance we observed (Figure 3E, bottom), this topographic relationship is analogous to the previous observation that SF tuning and binocularity are correlated positively (Nauhaus et al., 2016). These results suggest that the orthogonal organization of the SF and OD maps may be initialized by the spatial organization of the ON-OFF angle and distance in the bottom-up projections.

A Developmental Model of Cortical Maps

To explain how cortical tunings could be determined by the ON-OFF profiles, we carried out a model simulation of the development of the retino-cortical pathway (Figures 4 and S2). According to previous observations that the thalamocortical projections from the contralateral eye arrive at V1 layer 4 ahead of those from the ipsilateral pathway (Albus and Wolf, 1984; Crair et al., 1998), we implemented a simplified developmental model of binocular retino-cortical circuits (Figure 4A; see Figure S2A for details). In this scenario, the layout of diverse cortical tuning maps was initially seeded by the structure of contralateral retinal mosaics. The orthogonal organization of contralateral RGC mo-

saics (Figure 2) is mirrored onto the V1 surface, and the synaptic weights of ipsilateral feedforward projections are then updated to match the cortical tuning seeded by the contralateral projections (Figure 4A).

Previously, the Paik-Ringach model suggested that the receptive field of a V1 neuron is generated from the sum of receptive fields of the local RGC that provides feedforward afferents, and the PO of the V1 neuron is constrained by the ON-OFF angle of retinal inputs (Figure 4B). Here, expanding this developmental principle of orientation maps, we propose that the ON-OFF distance of RGC mosaics can also induce OD and the SF map. First, variation of the distance between neighboring ON and OFF RGCs modulates the degree of overlap between ON and OFF receptive field subregions, which varies the sum of neural responses to ON and OFF stimulus in contralateral afferents. This induces competition between contralateral and ipsilateral afferents, resulting in a periodic pattern of OD (Figure 4C; see Figure S2 for details). Second, in the binocular region, intermingling of both contralateral and ipsilateral inputs with different spatial phases of the receptive field induces a preference to higher SF than that in the monocular region (Figure 4D; see Figure S3 for details).

As a result, our developmental model shows how diverse cortical tunings can be initiated by retinal mosaics; the PO is seeded by the ON-OFF angle, while the OD and SF tuning are seeded by the ON-OFF distance. From the model simulation with mosaic data observed in cats and monkeys, we also found that the orthogonal organization between diverse cortical tunings was successfully generated in all functional maps achieved from the tested mosaic data (Figure 4E; PO- Δ OD; $OI = 4.75 \pm 2.36$, fitted to a von Mises distribution, $\mu = 87.7^\circ$, $\kappa = 1.2$, Δ PO- Δ SF; $OI = 4.62 \pm 3.85$, fitted to a von Mises distribution, $\mu = 86.9^\circ$, $\kappa = 0.77$). These results suggest that the orthogonal relationships among cortical tunings may stem from the projection of the orthogonal structure in the retina.

DISCUSSION

Our findings suggest that the orthogonal organization in V1 can originate from the spatial organization of the ON-OFF receptive fields in the bottom-up projections. We showed that an orthogonal relationship of sensory modules exists in the retinal mosaics and that this can be mirrored to V1 to initiate the clustered topography of higher visual areas in the brain. These results imply that spatially organized input from the periphery initially provides a common framework for functional architectures in the visual cortex, which could be refined by the recurrent and feedback cortical activities through subsequent developmental stages.

The present scope of our model is limited to explaining how retinal inputs can provide the “initial” blueprint for each functional map. Accordingly, detailed biological components were simplified or omitted in the current model if they were not closely related to the core mechanism discussed here and thus would not significantly affect the biological plausibility of the model. In our model, we simplified the retina-lateral geniculate nucleus (LGN)-V1 pathway as retina-V1 projections based on the fact that each LGN relays the RGC input with approximately a one-

to-one connection, as observed in previous anatomical (Hamos et al., 1987) and physiological (Cleland et al., 1971a, 1971b; Masstronde, 1992) studies. In cats, it was reported that most LGN neurons receive feedforward inputs from a small number of RGCs and that the profile of each LGN receptive field is identical to that of a single RGC in most cases, implying that the activity of LGN neurons is mainly modulated by a single RGC. Similar results were also observed in macaques (Schein and de Monasterio, 1987). Although LGN neurons are observed to receive feedforward inputs from multiple RGCs (Bloomfield et al., 1987; Hickey and Guillery, 1979), a recent study (Martinez et al., 2014) showed that the receptive fields of LGN neurons observed in experiments are mainly determined by a couple of ON and OFF RGCs around the center of the convergence (Alonso et al., 2006; Tavazoie and Reid, 2000) and are well matched with those predicted by the statistical wiring model (Ringach, 2004, 2007). Furthermore, our model simulations show that the orthogonal organization of the cortical map would remain consistent even when LGN neurons receive feedforward inputs from multiple RGCs. Simulations of the retino-cortical projection of various convergence ranges reveal that the orthogonal organization of the ON-OFF angle and distance remains consistent even with variation of the convergence range if neuronal tuning is predominantly determined by a couple of ON and OFF RGCs near the center of the convergence mapping in the retinal space (Figures S4A–S4C), as observed experimentally (Alonso et al., 2006; Tavazoie and Reid, 2000).

It must be noted that our simplification of the model by removing a detailed layered structure of the dorsal LGN (dLGN) in the retina-dLGN-V1 pathway does not sacrifice the biological plausibility of the main findings, and the addition of more realistic dLGN layers to the model does not affect our conclusion. The rationale of our simplification of the model by removing the dLGN layers is that different retina-dLGN-V1 pathways invade V1 at different developmental stages and that the initial blueprint of cortical maps can be dominantly initiated from a single feed-forward pathway, as we modeled. Among diverse pathways, the contralateral magnocellular pathway via layer 1 of the dLGN appears to contribute predominantly to early V1 organization, in which orientation selectivity in V1 is observed initially (Ghosh and Shatz, 1992; Mooser et al., 2004; Shatz and Luskin, 1986). Specifically, it was reported that orientation selectivity of the primary visual cortex in cats is observed between developmental stages E57 and P0, during which both magnocellular and parvocellular pathways are connected to V1 layer 4. However, orientation selectivity is observed only in sublayer 4C α , where the magnocellular pathway is predominantly connected. Furthermore, cortical cells in V1 layer 2/3 connected to the parvocellular pathway are not even completely migrated until postnatal week 3. Thus, it is reasonable to infer that the magnocellular thalamocortical input is the only source when orientation selectivity is observed initially. Our current model describes this very early stage of development assuming that the RGC mosaics of this single class are the only source when the initial layout of the functional maps is seeded. As a result, the model suggests that the orientation map can emerge from early magnocellular connectivity and that it is then refined by parvocellular connectivity after eye opening. In successive works, further analysis with

more complicated models may reveal the detailed mechanism by which these two pathways contribute to the development of functional maps.

Additional analysis with our extended simulations illustrates that the orthogonal organization of the cortical map would remain consistent when wirings via LGN layers are included in the model. When we measured the ON-OFF angle and distance in cortical receptive fields with a modified model simulation with the LGN layer added, the results show that orthogonal organizations remain consistent even when an additional LGN layer is implemented in the model (Figures S4D–S4F). This occurs because the ON/OFF topology of V1 neurons is consistently restricted by the local ON and OFF RGC mosaics, as it is in the retinotopic projections. Overall, our simplified model of the visual cortex represents the early developmental stage of the visual pathway to provide insight into our understanding of the developmental principles of multiple functional maps. However, it is obvious that the dynamic refinement of the recurrent and feedback circuits from the cortical activity and from visual experience is also a critical factor modifying the layout of functional maps (Craig et al., 1998; Thompson et al., 2016). Therefore, to understand the complete developmental process of the cortical circuits, additional components of the cortical circuit activity, such as cross-orientation suppression (Koch et al., 2016), must also be considered in future studies.

It should also be noted that the key idea of our model that the multiple functional maps and their correlated organizations may originate simultaneously via retinal input is also supported by a previous study showing that retinal activity in the early developmental stage is necessary for the development of an orientation map (Chapman and Gödecke, 2000). This study showed that the orientation map does not develop under a blockade of ON-center retinal ganglion cell activity during postnatal days 28–52, during which the orientation selectivity of neurons is observed to develop under normal conditions. Intriguingly, weak orientation selectivity was observed when they only blocked the ON-center retinal ganglion cell activity for half of the day. From this observation, the authors suggested that the presence of normal activity patterns for only half of each day is sufficient for orientation tuning to develop, and that ON-center RGC activity is necessary for the development of orientation maps.

Regarding the universality of our retinal origin model, it is arguable whether our model can also explain the development of randomly arranged neural tuning in the rodent V1, termed a salt-and-pepper map. In our recent study (Jang et al., 2020), we addressed this issue by showing that the retina-to-cortex sampling ratio is the key factor determining the organization of columnar and salt-and-pepper patterns in the visual cortex across species. From an analysis of retinal and cortical data from eight mammalian species, we find that cortical organization is predictable by a single factor: the retino-cortical mapping ratio. Groups of species with or without columnar clustering are distinguished by the feedforward sampling ratio, and model simulations with controlled mapping conditions reproduce both organization types. Predictions from the Nyquist theorem explain this parametric division of the patterns with high accuracy. Thus, our retinal origin model can readily explain both columnar

and salt-and-pepper organization types in various species with the same principle discussed above.

Notably, a previous study (Basole et al., 2003) suggested that combinations of features that are encoded in V1 neurons cannot be simply correspondent to the intersection of independent multiple feature maps but rather should be considered in terms of a single energy map because all of the features are systematically interdependent. However, it must be noted that these results do not reject the existence of multiple feature maps or the presence of a spatial correlation of multiple feature maps and are thus not contradictory to our model. Instead, these findings can also be consistent with our key assumption that multiple feature tunings develop from a single source—i.e., the spatial organization of ON and OFF RGC projections. We show that the results reported in the paper can be reproduced by our model by considering the spatiotemporal receptive fields of ON and OFF RGCs, particularly with a temporal delay between the ON and OFF responses (Figures S4G–S4J). Specifically, our model with the spatiotemporal receptive fields also predicts that when the bar stimulus moves along non-orthogonal axes, the preferred feature will be measured differently across different speeds of stimuli. Thus, the idea that multiple functional tunings should be considered in terms of a single energy map rather than the intersection of independent multiple feature maps is not contradictory but rather supportive of our model that multiple functional maps are interdependent and should be considered as maps developed by a single constraint, the retinal mosaic.

Our results imply that the current model can provide a framework for early organizations of the visual cortex for efficient coding, as suggested in previous model studies. For example, the Petitot-Citti-Sarti model (Petitot and Tondut, 1999; Sarti et al., 2008) suggests that the long-range horizontal connections between orientation columns preferring a similar orientation are the key factors accomplishing efficient coding in V1. Regarding this issue, we recently reported that these orientation-specific horizontal connections can be initiated by the retinal structure transferred by asynchronous ON and OFF retinal waves (Kim et al., 2020). Our model suggests that long-range orientation-specific horizontal connections could arise spontaneously by retinal projection, originating from spatiotemporally structured feedforward activities generated from spontaneous retinal waves. These findings overall suggest that functional maps and neuronal wirings for efficient coding, such as long-range connections, can arise spontaneously by retinal projection in the early developmental stage and that our model provides broader insight into not only the developmental mechanism of functional circuits in V1 but also the biological strategies of circuit organization for the efficient processing of sensory information.

In summary, our study suggests that spatially organized input from the periphery may provide a common framework for various functional architectures in the visual cortex. This common anatomical substrate results in the uniform representation of combinations of sensory modules by organizing a correlated topography of diverse visual tunings. Overall, our results suggest that the structure of the periphery with simple feedforward wiring can provide the beginnings of a mechanism by which the initial circuitry for the visual function is assembled.

STAR METHODS

Detailed methods are provided in the online version of this paper and include the following:

- KEY RESOURCES TABLE
- RESOURCE AVAILABILITY
 - Lead Contact
 - Materials Availability
 - Data and Code Availability
- EXPERIMENTAL MODEL AND SUBJECT DETAILS
- METHOD DETAILS
 - Analysis of RGC mosaics
 - Analysis of multi-electrode recordings
 - Design of developmental model
 - Connectivity and receptive field models
 - Nonlinear response curve of a single neuron
 - Binocular development and Hebbian plasticity
 - Measurement of cortical functional maps
- QUANTIFICATION AND STATISTICAL ANALYSIS

SUPPLEMENTAL INFORMATION

Supplemental Information can be found online at <https://doi.org/10.1016/j.celrep.2020.108581>.

ACKNOWLEDGMENTS

We are grateful to Jose-Manuel Alonso for sharing receptive field data on the cat visual cortex. We also thank Dario Ringach, Matteo Carandini, Daeyeol Lee, and Andrea Benucci for providing comments in the early stages of this study. This work was supported by a National Research Foundation of Korea (NRF) grant funded by the Korean government (nos. NRF-2019R1A2C4069863 and NRF-2019M3E5D2A01058328) (to S.-B.P.).

AUTHOR CONTRIBUTIONS

Conceptualization, M.S., J.J., and S.-B.P.; Methodology, M.S., J.J., and S.-B.P.; Software, M.S. and J.J.; Validation, M.S., J.J., and S.-B.P.; Formal Analysis, M.S., J.J., G.K., and S.-B.P.; Investigation, M.S. and J.J.; Resources, S.-B.P.; Writing – Original Draft, M.S., J.J., and S.-B.P.; Writing – Review & Editing, M.S., J.J., and S.-B.P.; Visualization, M.S., J.J., and S.-B.P.; Supervision, S.-B.P.; Funding Acquisition, S.-B.P.

DECLARATION OF INTERESTS

The authors declare no competing interests.

Received: June 11, 2020

Revised: October 22, 2020

Accepted: December 9, 2020

Published: January 5, 2021

SUPPORTING CITATIONS

The following references appear in the Supplemental Information: Chichilnisky and Kalmar (2002); Crair et al. (1997b); Derrington (1984); LeVay et al. (1978); Ohzawa et al. (1996); Shatz (1983); Suematsu et al. (2013).

REFERENCES

Albus, K., and Wolf, W. (1984). Early post-natal development of neuronal function in the kitten's visual cortex: a laminar analysis. *J. Physiol.* 348, 153–185.

- Alonso, J.-M., Yeh, C.-I., Weng, C., and Stoelzel, C. (2006). Retinogeniculate connections: a balancing act between connection specificity and receptive field diversity. *Prog. Brain Res.* 154, 3–13.
- Balasubramanian, V., and Sterling, P. (2009). Receptive fields and functional architecture in the retina. *J. Physiol.* 587, 2753–2767.
- Basole, A., White, L.E., and Fitzpatrick, D. (2003). Mapping multiple features in the population response of visual cortex. *Nature* 423, 986–990.
- Blasdel, G.G., and Salama, G. (1986). Voltage-sensitive dyes reveal a modular organization in monkey striate cortex. *Nature* 321, 579–585.
- Bloomfield, S.A., Hamos, J.E., and Sherman, S.M. (1987). Passive cable properties and morphological correlates of neurones in the lateral geniculate nucleus of the cat. *J. Physiol.* 383, 653–692.
- Brown, S.P., He, S., and Masland, R.H. (2000). Receptive field microstructure and dendritic geometry of retinal ganglion cells. *Neuron* 27, 371–383.
- Chapman, B., and Gödecke, I. (2000). Cortical cell orientation selectivity fails to develop in the absence of ON-center retinal ganglion cell activity. *J. Neurosci.* 20, 1922–1930.
- Chichilnisky, E.J., and Kalmar, R.S. (2002). Functional asymmetries in ON and OFF ganglion cells of primate retina. *J. Neurosci.* 22, 2737–2747.
- Chung, S., and Ferster, D. (1998). Strength and orientation tuning of the thalamic input to simple cells revealed by electrically evoked cortical suppression. *Neuron* 20, 1177–1189.
- Cleland, B.G., Dubin, M.W., and Levick, W.R. (1971a). Simultaneous recording of input and output of lateral geniculate neurones. *Nat. New Biol.* 231, 191–192.
- Cleland, B.G., Dubin, M.W., and Levick, W.R. (1971b). Sustained and transient neurones in the cat's retina and lateral geniculate nucleus. *J. Physiol.* 217, 473–496.
- Craig, M.C., Ruthazer, E.S., Gillespie, D.C., and Stryker, M.P. (1997a). Ocular dominance peaks at pinwheel center singularities of the orientation map in cat visual cortex. *J. Neurophysiol.* 77, 3381–3385.
- Craig, M.C., Ruthazer, E.S., Gillespie, D.C., and Stryker, M.P. (1997b). Relationship between the ocular dominance and orientation maps in visual cortex of monocularly deprived cats. *Neuron* 19, 307–318.
- Craig, M.C., Gillespie, D.C., and Stryker, M.P. (1998). The role of visual experience in the development of columns in cat visual cortex. *Science* 279, 566–570.
- Croner, L.J., and Kaplan, E. (1995). Receptive fields of P and M ganglion cells across the primate retina. *Vision Res.* 35, 7–24.
- Derrington, A.M. (1984). Development of spatial frequency selectivity in striate cortex of vision-deprived cats. *Exp. Brain Res.* 55, 431–437.
- Douglas, R.J., Koch, C., Mahowald, M., Martin, K.A., and Suarez, H.H. (1995). Recurrent excitation in neocortical circuits. *Science* 269, 981–985.
- Ferster, D., Chung, S., and Wheat, H. (1996). Orientation selectivity of thalamic input to simple cells of cat visual cortex. *Nature* 380, 249–252.
- Gauthier, J.L., Field, G.D., Sher, A., Greschner, M., Shlens, J., Litke, A.M., and Chichilnisky, E.J. (2009a). Receptive fields in primate retina are coordinated to sample visual space more uniformly. *PLOS Biol.* 7, e1000063.
- Gauthier, J.L., Field, G.D., Sher, A., Shlens, J., Greschner, M., Litke, A.M., and Chichilnisky, E.J. (2009b). Uniform signal redundancy of parasol and midget ganglion cells in primate retina. *J. Neurosci.* 29, 4675–4680.
- Ghosh, A., and Shatz, C.J. (1992). Pathfinding and target selection by developing geniculocortical axons. *J. Neurosci.* 12, 39–55.
- Hamos, J.E., Van Horn, S.C., Raczkowski, D., and Sherman, S.M. (1987). Synaptic circuits involving an individual retinogeniculate axon in the cat. *J. Comp. Neurol.* 259, 165–192.
- Hickey, T.L., and Guillory, R.W. (1979). Variability of laminar patterns in the human lateral geniculate nucleus. *J. Comp. Neurol.* 183, 221–246.
- Horton, J.C., and Adams, D.L. (2005). The cortical column: a structure without a function. *Philos. Trans. R. Soc. Lond. B Biol. Sci.* 360, 837–862.
- Hübener, M., Shoham, D., Grinvald, A., and Bonhoeffer, T. (1997). Spatial relationships among three columnar systems in cat area 17. *J. Neurosci.* 17, 9270–9284.
- Issa, N.P., Trepel, C., and Stryker, M.P. (2000). Spatial frequency maps in cat visual cortex. *J. Neurosci.* 20, 8504–8514.
- Jang, J., and Paik, S.-B. (2017). Interlayer repulsion of retinal ganglion cell mosaics regulates spatial organization of functional maps in the visual cortex. *J. Neurosci.* 37, 12141–12152.
- Jang, J., Song, M., and Paik, S.-B. (2020). Retino-cortical mapping ratio predicts columnar and salt-and-pepper organization in mammalian visual cortex. *Cell Rep.* 30, 3270–3279.e3.
- Jin, J., Wang, Y., Swadlow, H.A., and Alonso, J.M. (2011). Population receptive fields of ON and OFF thalamic inputs to an orientation column in visual cortex. *Nat. Neurosci.* 14, 232–238.
- Kim, J., Song, M., Jang, J., and Paik, S.-B. (2020). Spontaneous Retinal Waves Can Generate Long-Range Horizontal Connectivity in Visual Cortex. *J. Neurosci.* 40, 6584–6599.
- Koch, E., Jin, J., Alonso, J.M., and Zaidi, Q. (2016). Functional implications of orientation maps in primary visual cortex. *Nat. Commun.* 7, 13529.
- Kremkow, J., Jin, J., Wang, Y., and Alonso, J.M. (2016). Principles underlying sensory map topography in primary visual cortex. *Nature* 533, 52–57.
- Lansdman, C.E., and Ts'o, D.Y. (2002). Color processing in macaque striate cortex: relationships to ocular dominance, cytochrome oxidase, and orientation. *J. Neurophysiol.* 87, 3126–3137.
- Lee, K.-S., Huang, X., and Fitzpatrick, D. (2016). Topology of ON and OFF inputs in visual cortex enables an invariant columnar architecture. *Nature* 533, 90–94.
- LeVay, S., Stryker, M.P., and Shatz, C.J. (1978). Ocular dominance columns and their development in layer IV of the cat's visual cortex: a quantitative study. *J. Comp. Neurol.* 179, 223–244.
- LeVay, S., Connolly, M., Houde, J., and Van Essen, D.C. (1985). The complete pattern of ocular dominance stripes in the striate cortex and visual field of the macaque monkey. *J. Neurosci.* 5, 486–501.
- Martinez, L.M., Molano-Mazón, M., Wang, X., Sommer, F.T., and Hirsch, J.A. (2014). Statistical wiring of thalamic receptive fields optimizes spatial sampling of the retinal image. *Neuron* 81, 943–956.
- Mastronarde, D.N. (1992). Nonlagged relay cells and interneurons in the cat lateral geniculate nucleus: receptive-field properties and retinal inputs. *Vis. Neurosci.* 8, 407–441.
- Mooser, F., Bosking, W.H., and Fitzpatrick, D. (2004). A morphological basis for orientation tuning in primary visual cortex. *Nat. Neurosci.* 7, 872–879.
- Movshon, J.A., Thompson, I.D., and Tolhurst, D.J. (1978). Receptive field organization of complex cells in the cat's striate cortex. *J. Physiol.* 283, 79–99.
- Nauhaus, I., and Nielsen, K.J. (2014). Building maps from maps in primary visual cortex. *Curr. Opin. Neurobiol.* 24, 1–6.
- Nauhaus, I., Nielsen, K.J., Disney, A.A., and Callaway, E.M. (2012). Orthogonal micro-organization of orientation and spatial frequency in primate primary visual cortex. *Nat. Neurosci.* 15, 1683–1690.
- Nauhaus, I., Nielsen, K.J., and Callaway, E.M. (2016). Efficient receptive field tiling in primate V1. *Neuron* 91, 893–904.
- Ohzawa, I., DeAngelis, G.C., and Freeman, R.D. (1996). Encoding of binocular disparity by simple cells in the cat's visual cortex. *J. Neurophysiol.* 75, 1779–1805.
- Paik, S.-B., and Ringach, D.L. (2011). Retinal origin of orientation maps in visual cortex. *Nat. Neurosci.* 14, 919–925.
- Paik, S.-B., and Ringach, D.L. (2012). Link between orientation and retinotopic maps in primary visual cortex. *Proc. Natl. Acad. Sci. USA* 109, 7091–7096.
- Petitot, J., and Tondut, Y. (1999). Vers une neurogéométrie. Vibrations corticales, structures de contact et contours subjectifs modaux. *Math. Sci. Hum.* 145, 5–101.
- Rhoades, C.E., Shah, N.P., Manookin, M.B., Brackbill, N., Kling, A., Goetz, G., Sher, A., Litke, A.M., and Chichilnisky, E.J. (2019). Unusual physiological

- properties of smooth monostratified ganglion cell types in primate retina. *Neuron* 103, 658–672.e6.
- Ringach, D.L. (2004). Haphazard wiring of simple receptive fields and orientation columns in visual cortex. *J. Neurophysiol.* 92, 468–476.
- Ringach, D.L. (2007). On the origin of the functional architecture of the cortex. *PLOS ONE* 2, e251.
- Ruderman, D.L., and Bialek, W. (1994). Statistics of natural images: scaling in the woods. *Phys. Rev. Lett.* 73, 814–817.
- Sailamul, P., Jang, J., and Paik, S.-B. (2017). Synaptic convergence regulates synchronization-dependent spike transfer in feedforward neural networks. *J. Comput. Neurosci.* 43, 189–202.
- Sarti, A., Citti, G., and Petitot, J. (2008). The symplectic structure of the primary visual cortex. *Biol. Cybern.* 98, 33–48.
- Schein, S.J., and de Monasterio, F.M. (1987). Mapping of retinal and geniculocal neurons onto striate cortex of macaque. *J. Neurosci.* 7, 996–1009.
- Sejnowski, T.J. (1977). Storing covariance with nonlinearly interacting neurons. *J. Math. Biol.* 4, 303–321.
- Shatz, C.J. (1983). The prenatal development of the cat's retinogeniculate pathway. *J. Neurosci.* 3, 482–499.
- Shatz, C.J., and Luskin, M.B. (1986). The relationship between the geniculocortical afferents and their cortical target cells during development of the cat's primary visual cortex. *J. Neurosci.* 6, 3655–3668.
- Soodak, R.E. (1987). The retinal ganglion cell mosaic defines orientation columns in striate cortex. *Proc. Natl. Acad. Sci. USA* 84, 3936–3940.
- Suematsu, N., Naito, T., Miyoshi, T., Sawai, H., and Sato, H. (2013). Spatiotemporal receptive field structures in retinogeniculate connections of cat. *Front. Syst. Neurosci.* 7, 103.
- Swindale, N.V., Shoham, D., Grinvald, A., Bonhoeffer, T., and Hübener, M. (2000). Visual cortex maps are optimized for uniform coverage. *Nat. Neurosci.* 3, 822–826.
- Tavazoie, S.F., and Reid, R.C. (2000). Diverse receptive fields in the lateral geniculate nucleus during thalamocortical development. *Nat. Neurosci.* 3, 608–616.
- Thompson, A.D., Picard, N., Min, L., Fagiolini, M., and Chen, C. (2016). Cortical feedback regulates feedforward retinogeniculate refinement. *Neuron* 91, 1021–1033.
- Van Hooser, S.D. (2007). Similarity and diversity in visual cortex: is there a unifying theory of cortical computation? *Neuroscientist* 13, 639–656.
- Vidne, M., Ahmadian, Y., Shlens, J., Pillow, J.W., Kulkarni, J., Litke, A.M., Chichilnisky, E.J., Simoncelli, E., and Paninski, L. (2012). Modeling the impact of common noise inputs on the network activity of retinal ganglion cells. *J. Comput. Neurosci.* 33, 97–121.
- Wässle, H., Boycott, B.B., and Illing, R.-B. (1981). Morphology and mosaic of on- and off-beta cells in the cat retina and some functional considerations. *Proc. R. Soc. Lond. B Biol. Sci.* 212, 177–195.
- Weliky, M., Bosking, W.H., and Fitzpatrick, D. (1996). A systematic map of direction preference in primary visual cortex. *Nature* 379, 725–728.
- Xu, X., Bosking, W.H., White, L.E., Fitzpatrick, D., and Casagrande, V.A. (2005). Functional organization of visual cortex in the prosimian bush baby revealed by optical imaging of intrinsic signals. *J. Neurophysiol.* 94, 2748–2762.
- Zhan, X.J., and Troy, J.B. (2000). Modeling cat retinal beta-cell arrays. *Vis. Neurosci.* 17, 23–39.

STAR★METHODS

KEY RESOURCES TABLE

REAGENT or RESOURCE	SOURCE	IDENTIFIER
Software and Algorithms		
MATLAB 2017a	MathWorks	RRID:SCR_001622

RESOURCE AVAILABILITY

Lead Contact

Further information and requests for resources should be directed to and will be fulfilled by the Lead Contact, Se-Bum Paik (sbpaik@kaist.ac.kr).

Materials Availability

This study did not generate new unique reagents.

Data and Code Availability

Data supporting the findings of this study are available in the main text and [Supplemental Information Appendix](#). The associated code and scripts reproducing all of the results in the paper are available from the corresponding author on reasonable request.

EXPERIMENTAL MODEL AND SUBJECT DETAILS

The functional maps in cats (5 cats, unknown sex, aged 2–5 months) are from [Crair et al. \(1997a\)](#), [Hübener et al. \(1997\)](#), and [Issa et al. \(2000\)](#) for orientation and ocular dominance maps, and from [Hübener et al. \(1997\)](#), [Issa et al. \(2000\)](#), and [Swindale et al. \(2000\)](#) for spatial frequency maps. The functional maps in the monkeys (5 monkeys, 3 male, 1 female and 1 unknown sex, unknown age) are from [Landisman and Ts'o \(2002\)](#) and [Nauhaus et al. \(2012, 2016\)](#) for orientation maps; [Landisman and Ts'o \(2002\)](#) and [Nauhaus et al. \(2016\)](#) for ocular dominance maps; and [Nauhaus et al. \(2012, 2016\)](#) for spatial frequency maps. Orientation and ocular dominance maps in galago (1 galago, unknown sex, unknown age) are from [Xu et al. \(2005\)](#). Orientation map in ferret (1 ferret, unknown sex, unknown age) are from [Weliky et al. \(1996\)](#). The multielectrode data of the cat visual cortex (1 cat, male, aged 6–12 months) are from [Kremkow et al. \(2016\)](#). The retinal ganglion cell mosaics in two cats (2 cat, unknown sex, unknown age) are from [Wässle et al. \(1981\)](#) and [Zhan and Troy \(2000\)](#). The retinal ganglion cell mosaics in monkeys (4 Monkeys, unknown sex, unknown age) are from [Gauthier et al. \(2009a, 2009b\)](#), [Rhoades et al. \(2019\)](#), and [Vidne et al. \(2012\)](#).

METHOD DETAILS

Analysis of RGC mosaics

We modeled the cortical receptive fields by sampling the receptive fields of local ON and OFF RGCs. We assumed that the RGCs are statistically wired to cortical space with a 2D Gaussian, where the sigma of synaptic weighting was set to 0.16–0.18 times the expected average lattice distance of OFF RGC mosaics, d_{OFF} ([Paik and Ringach, 2011](#); [Sailamul et al., 2017](#)). The local receptive field was calculated at each vertex of a rectangular grid with a spacing distance of $0.1d_{OFF}$ in the RGC mosaics. We analyzed four mosaics of the receptive field and two mosaics of the cell body of ON/OFF RGCs based on a report that the receptive field center, dendritic field center and soma of a single RGC are tightly clustered on the retinal surface ([Brown et al., 2000](#)).

The receptive fields of RGCs and V1 neurons were defined as a center-surround model of 2D Gaussian and their linear sum, respectively. The size and the amplitude of the surrounding region were set to 3 and 0.55 times that of the center region. The ON-OFF angle and distance were measured between the center-of-mass of the modeled ON and OFF receptive fields and then the resultant maps were smoothed using a 2D Gaussian kernel with sigma of $0.6-1d_{OFF}$.

The orthogonality index (OI) of a tuning curve was measured as follows:

$$\mu = \sum_{\theta=0}^{2\pi} (\exp(i\theta) \times r_\theta)$$

$$OI = |\mu| \times \sin(\arg(\mu)) / \bar{r}$$

where θ indicates each angle, r_θ indicates the response for each angle, \bar{r} indicates the mean response. O/I becomes 0 for a uniform tuning curve and increases as the orthogonal bias becomes stronger. The significance of the orthogonal bias was tested by comparing O/I with that measured from the shuffled distribution of ON-OFF angle and distance.

Analysis of multi-electrode recordings

The multi-electrode data recorded from the cats were provided by Jose-Manuel Alonso (Kremkow et al., 2016) for the analysis in Figure 3. To remove high-frequency spatial noise, the receptive fields were filtered by a low-pass Fermi filter in the frequency domain. The filter was designed according to

$$f = 1 / \left(\exp\left(\frac{\omega - \mu}{K\mu}\right) + 1 \right)$$

, where μ is the threshold of the frequency (4 cpd) and K is the smoothness coefficient. The ON-OFF angle was estimated from the Fourier transform $\Psi(\omega)$ of the receptive fields (Paik and Ringach, 2011). It is defined as $\arg(\mu)/2$, where

$$\mu = \int |\Psi(\omega)| \omega \exp(2i \arg(\omega)) d\omega / \int |\Psi(\omega)| d\omega$$

Samples for which either the ON or OFF subregion is entirely canceled by the other component were excluded. The ON-OFF distance was defined as the distance between the center of the ON and OFF subregions. The location of the center of the ON and OFF subregions was defined as the strongest peak of each subregion. For multiple subregion samples, the largest subregion was chosen for analysis.

Design of developmental model

The simulations were performed based on the statistical wiring model (Ringach, 2004, 2007). Diverse cortical tunings were simulated from the model cortical neuronal response to drifting grating received from retinal ganglion cells. Drifting grating, designed as a sine function of twenty different spatial frequencies (0.5–8 cycles/degree) and twenty orientations (0– π), was given to binocular retinal mosaics. All simulations and statistical tests were performed using MATLAB R2017a. We summarized the detailed algorithm and the parameters used in the simulations in [Supplemental Information](#).

Connectivity and receptive field models

At the initial stage of development, we assumed that the RGCs are statistically wired to cortical space with two-dimensional Gaussian function with a standard deviation of σ_{con} .

$$w_{ij} = \frac{W_{init}}{\sigma_{con}\sqrt{2\pi}} \exp\left(-\frac{(d_{ij} + \eta_{V1j})^2}{2\sigma_{con}^2}\right)$$

Here, w_{ij} represents the synaptic weighting between i^{th} RGC and j^{th} cortical sites, where W_{init} is the initial connection weight. For realistic retinotopic projection, we added zero mean two-dimensional Gaussian noise, η_{V1j} , with a standard deviation of σ_R . The receptive fields of RGCs and V1 neurons were defined as a center-surround model of 2D Gaussian and their linear sum, respectively. The standard deviation of the surrounding region was set to three times that of the center region (Croner and Kaplan, 1995).

$$\Psi_{i, RGC} = \pm \left(\frac{1}{\sigma\sqrt{2\pi}} \exp\left(-\frac{r_i^2}{2\sigma_{RGC}^2}\right) - \frac{1}{3\sigma\sqrt{2\pi}} \exp\left(-\frac{r_i^2}{18\sigma_{RGC}^2}\right) \right) (+ : ON\ cell, - : OFF\ cell)$$

$$\Psi_{j, V1} = \sum_i w_{ij} \cdot \Psi_i^{RGC}$$

Here, $\Psi_{i, RGC}$ is the receptive field of i^{th} RGC, and $\Psi_{j, V1}$ is for the j^{th} cortical site where r_i is a distance vector from the center of i^{th} RGC to each position of the visual field. In this case, $\sigma_{ON,RGC}$ and $\sigma_{OFF,RGC}$ were set as $(1 + \alpha)d/2$ and $d/2$ to satisfy the condition that the receptive fields of ON and OFF RGC mosaics cover all of the visual field (Balasubramanian and Sterling, 2009), where α is the lattice distance ratio (0.108 ± 0.003 in cat data and 0.120 ± 0.053 in monkey data; Figure S1D).

Nonlinear response curve of a single neuron

The response curves of RGCs and V1 neurons were designed based on the linear-nonlinear model, which shows a normalized response to visual input S through a sigmoidal kernel

$$A_{i, RGC}(S) = \left(1 + \exp\left(-\frac{\Psi_{i, RGC} \cdot S}{\delta_{RGC}}\right) \right)^{-1}$$

$$A_{j, V1}(S) = \left(1 + \exp\left(-\frac{I - 0.5}{\delta_{V1}} \right) \right)^{-1}$$

$$I = \sum_i w_{ij} \cdot R_{i, RGC}$$

where $A_{i, RGC}(S)$ and $A_{j, V1}(S)$ are the response of i^{th} RGC and j^{th} cortical cell for visual stimuli S . Here, δ stands for nonlinearity of the sigmoidal response function. All the parameter details are shown in [Table S1](#) (\cdot denotes a Hadamard product).

Binocular development and Hebbian plasticity

In our binocular development model, the development of connections between contralateral RGCs and V1 neurons were first simulated, and then the ipsilateral connections were allowed to develop (for details, see [Figure 4](#)). During the development of contralateral connections, a random noise activity was provided as a spontaneous retinal activity. Then, during the binocular development stage, natural-like filtered noise images ([Ruderman and Bialek, 1994](#)) were provided to both retinal mosaics as a simulation of external visual input.

The synaptic weights were updated following a simple covariance rule ([Sejnowski, 1977](#)) as follows

$$\Delta w_{ij} = \begin{cases} \epsilon \left(R_{V1j} - \bar{R}_{V1j} \right) \left(R_{RGCi} - \bar{R}_{RGCi} \right) & \text{if } w_{ij} < w_{lim} \\ 0 & \text{if } w_{ij} \geq w_{lim} \text{ OR } \sum_i w_{ij} \geq W_{lim} \end{cases}$$

$$\bar{R} = \frac{1}{\tau} \int_{-\infty}^t R \cdot e^{(t'-t)/\tau} dt'$$

where the learning threshold \bar{R} is defined as the average value of the current response of the cortical cell. The τ represents a time constant showing how rapidly the threshold changes. The ϵ represents the learning rate, how fast the synaptic weights are updated. Note that we assumed that there is a limitation of resource, so both w_{ij} and $\sum_i w_{ij}$ have upper limit w_{lim} and W_{lim} . The development of both contra- and ipsilateral pathways were simulated with white noise inputs for 10,000 frames.

Measurement of cortical functional maps

The preferred orientation (θ_{OP}) of the calculated V1 receptive field was estimated from its Fourier transform $\Psi(\omega)$. θ_{OP} was defined as $\theta_{Pref} = \arg(\mu)/2$, where

$$\mu = \int |\Psi(\omega)| \omega | \exp(2i \arg(\omega)) d\omega / \int |\Psi(\omega)| d\omega$$

The ocular dominance was calculated as the relative strength of the mean cortical response \bar{R}_{V1} , to visual stimulus S , given to contra- and ipsilateral RGCs.

$$OD = \frac{\bar{R}_{V1}(S_{contra}) - \bar{R}_{V1}(S_{ipsi})}{\bar{R}_{V1}(S_{contra}) + \bar{R}_{V1}(S_{ipsi})}$$

To measure the spatial frequency, we computed the response of cortical cells to drifting gratings of various orientation and spatial frequency. The preferred spatial frequency was defined as the value of spatial frequency that induces the maximum response. To implement a realistic map-topography, each map was simulated from the hexagonal retinal mosaics with a realistic level of spatial noise in the cell position ([Paik and Ringach, 2011](#)) and all the simulated maps in the study were averaged from 20 repeated trials of simulation.

QUANTIFICATION AND STATISTICAL ANALYSIS

The Mann-Whitney U test was used to determine the significance of orthogonal bias of retinal mosaics ([Figure 2D](#)) and to determine the significance of the change of preferred orientation difference between contra- and ipsilateral afferents after the designed binocular development ([Figure S2I](#)). The bootstrap analysis was used to test the orthogonality bias of the model RGC mosaics, in which the orthogonality index of the original mosaics was compared to that of the shuffled distribution of the ON-OFF angle and distance ([Figure S1J](#)). Two-tailed t test was used to determine the significance of hexagonal peaks in measured RGC mosaic ([Figures S1B](#) and [S1C](#)). Pearson correlation coefficient (“corrcoef” function in MATLAB) was measured to determine the relationship between the functional tunings and ON-OFF angle/distance ([Figures 3C–3E](#), [S2G](#), and [S3E](#)). Sample sizes, statistical tests and p values are indicated in the text, figures, and figure legends. All the quantitative data are presented in mean \pm SD. The notation “N” represents the number of animals and “n” represents the number of the sample data points.